

See discussions, stats, and author profiles for this publication at: <https://www.researchgate.net/publication/5442329>

Metal Flux and Dynamic Speciation at (Bio)Interfaces. Part III: MHEDYN, a General Code for Metal Flux Computation; Application to Simple and Fulvic Complexants

ARTICLE in ENVIRONMENTAL SCIENCE AND TECHNOLOGY · APRIL 2008

Impact Factor: 5.33 · DOI: 10.1021/es071319n · Source: PubMed

CITATIONS

15

READS

32

5 AUTHORS, INCLUDING:



Davide Alemani

École Polytechnique Fédérale de Lausanne

19 PUBLICATIONS 267 CITATIONS

SEE PROFILE



Josep Galceran

Universitat de Lleida

117 PUBLICATIONS 1,950 CITATIONS

SEE PROFILE

Metal Flux and Dynamic Speciation at (Bio)Interfaces. Part III: MHEDYN, a General Code for Metal Flux Computation; Application to Simple and Fulvic Complexants

DAVIDE ALEMANI, JACQUES BUFFLE,*
AND ZESHI ZHANG

*CABE, Department of Inorganic, Analytical and Applied
Chemistry, Sciences II, 30 quai E. Ansermet, 1211 Geneva 4,
Switzerland*

JOSEP GALCERAN

*Department de Química, Universitat de Lleida, av. Rovira
Roure 191, 25198 Lleida, Spain*

BASTIEN CHOPARD

*Department of Computer Science, University of Geneva,
Switzerland*

*Received June 4, 2007. Revised manuscript received
November 30, 2007. Accepted December 6, 2007.*

Metal flux at consuming interfaces (e.g., sensors or microorganisms) is simulated in environmental multiligand systems using a new numerical code, MHEDYN (Multispecies Heterogeneous DYNamics), based on the lattice Boltzmann method. The attention is focused on the computation of the maximum flux of Cu(II), that is, the flux controlled by diffusion-reaction in solution, irrespective of processes occurring at the interface. In parts III and IV of this series, three types of typical environmental complexants are studied: (a) simple ligands (OH^- and CO_3^{2-}), (b) fulvic or humic substances including many sites with broadly varying rate constants, and (c) aggregates including a broad range of sizes and diffusion coefficients. Part III focuses on computations in the presence of simple ligands and fulvic/humic substances separately, and part IV discusses the case of aggregate complexes alone and the mixtures of all ligands in typical natural waters. These papers describe the dynamic contribution of the various types of sites for fulvic and aggregate Cu(II) complexes for the first time. Whenever possible, the metal fluxes computed by MHEDYN are compared with those given by another code, FLUXY, based on a fully different mathematical approach, and very good agreement between these codes is obtained. In all cases, MHEDYN computes the concentration profile of each complex and its time evolution, as well as the steady-state flux and the corresponding contribution of each complex to the flux. The metal fluxes can be computed at a planar consuming surface such as an organism or a sensor surface, in presence of an unlimited number of complexation reactions of the metal M, and for any metal/ligand concentration ratio, with values of the physicochemical parameters ranging over many orders of magnitude.

1. Introduction

Many biophysicochemical processes in aquatic systems are dynamic (1, 2). In particular, even though most metal bioavailability studies are presently based on the free ion activity model (FIAM) or the biotic ligand model (BLM), which assume that diffusion and chemical reactions in solution are very fast and, thus, are not rate limiting with respect to the transfer of metal through the consuming surface, it has been shown (3) that this latter assumption is often not fulfilled under natural conditions. In fact, the biouptake of metals by microorganisms may depend on hydrodynamics, metal transport in solution by diffusion and chemical kinetics of complex formation/dissociation, as well as metal transfer through the plasma membrane (4–6). The computation of metal flux, at consuming interfaces and in complicated environmental systems including many ligands, is a difficult task due to the many coupled dynamic physical and chemical processes. Theoretical concepts were developed a long time ago for metal flux at voltammetric electrodes in the presence of a single ligand (7, 8). Such concepts have been applied more recently to bioanalytical sensors and biouptake (6, 9, 10). Theories have also been extended recently to the case of solutions containing many ligands (L) (11–14), even though the case of ML_n ($n > 1$) complexes is only discussed in ref 14. In most cases, the ligands are supposed to be in excess compared to the total metal concentration. As far as computation codes are concerned, the situation of metal flux computation is at odds with that of thermodynamic distribution of metal complexes, for which a wealth of codes have been developed (15, 16). Even though the mathematical basis of metal flux computation in mixtures of many ligands is available (13, 17, 18), to our knowledge only one sufficiently user-friendly code has been published, FLUXY (19), which considers the wide range of chemical kinetics and diffusion coefficients operative in natural waters. FLUXY, however, has more limitations than MHEDYN, as explained in Section 2.

Parts III and IV (20) of this series of papers have two major goals: (i) to show how the new code MHEDYN (Multispecies Heterogeneous DYNamics), developed on the principles explained in refs 17 and 18, is applicable for transient and steady-state flux computations in complicated environmentally realistic mixtures of ligands; and (ii) to study the relative role of each individual natural complex on the steady-state metal flux at a consuming interface, such as an organism.

Natural complexants include various types of compounds, often with complicated properties (21). They can be classified into three categories (22, 23): (a) the so-called simple organic and inorganic ligands, such as OH^- , CO_3^{2-} , aminoacids, or oxalate, which are often present in large excess compared to transition and b metals. Their interactions with metals are largely controlled by simple electrostatic and covalent forces; (b) the organic biopolymers, in particular the humic/fulvic compounds; and (c) the colloidal particles and aggregates whose size range is 1–1000 nm, which include a significant fraction of inorganic solids such as clays or iron oxyhydroxide. Each type of complexant has its own specific properties that should be considered for correct computation of the metal flux. These aspects are discussed in detail in refs 22 and 23 and will not be discussed again here. In this paper (Part III), we describe the code (Section 2), and we focus on metal flux computations in the presence of simple and fulvic/humic complexants (Sections 3 and 4, respectively). Part IV (20) will study the flux of metal complexed by particles/aggregates and in complexant mixtures typical of freshwaters. Key

* Corresponding author telephone: ++41 22 3796053; fax: + 41 22 3796069; e-mail: Jacques.Buffle@cabe.unige.ch.

aspects related to simple and fulvic complexants are briefly summarized by the following properties: (a) simple complexants are small size compounds forming highly mobile complexes, often labile or semilabile, with weak-to-intermediate stability. Thus, their contribution to metal bioavailability in water may be limited by their low proportion in the whole of metal complexes. (b) Humics and fulvics are small polyelectrolytes (1–3 nm) with intermediate mobility, and they form metal complexes with widely varying stability and rate constants that strongly depend on the metal/ligand ratio under the test conditions. Thus, their contribution to the metal flux is expected to depend largely on this latter parameter.

The so-called maximum flux is always computed in Parts III and IV of this series. It is obtained when the interfacial process is so fast that the limiting factors to the flux are diffusion and chemical reactions in solution. This maximum flux is, thus, independent of the processes of metal transfer at the consuming interface. It only depends on the physical and chemical composition of the environmental medium. This maximum flux provides a limiting value of the flux that can be compared to the minimum flux (corresponding to the FIAM or BLM models), obtained when the transfer at the interface is the slowest process, that is, when no concentration gradient develops at the interface. The maximum flux is, thus, a complementary key information required to characterize an aquatic system with respect to bioavailability of metals and, consequently, to their ecotoxicology.

2. The Physical Model and the Computer Code

The general mathematical formulation and numerical algorithm of MHEDYN are described in detail in refs 17, 18, 24, and 25 and are summarized in the Supporting Information. Key assumptions are the following: it is assumed that the solution contains m types of ligands or complexing sites (iL , numbered $j = 1$ to m) which may form with M , either single 1/1 complexes, M/L , or successive complexes M/L_i , where i is the stoichiometric number of ligands iL in the complex. In addition, in all cases, (i) the initial solution is homogeneous and at equilibrium, and (ii) the bulk concentration of any species is at equilibrium and is independent of time. The boundary conditions related to each species at the consuming interface are the following: (a) free M is consumed at the interface, and its concentration $[M]^0$ on the solution side of the surface (superscript 0) is nil (Supporting Information eq S-9). This condition implies that the transfer rate of M through the interface is much faster than the diffusion/reaction of all M species in solution, that is, the flux in solution is the maximum possible flux; (b) iL does not cross the interface, (Supporting Information eq S-10); (c) M/L_i does not cross the interface, (Supporting Information eq S-11). The metal of a complex, however, is bioavailable after dissociation of M/L_i in the reaction–diffusion layer, near the interface; and (d) the flux is computed under conditions of finite diffusion, that is, the concentrations of all species at a finite distance (δ) of the consuming interface are assumed to be equal to those in the bulk solution. This corresponds to typical conditions in stirred natural waters (26). A value of $\delta = 20 \mu\text{m}$ is used in this paper and in most of Part IV. The value $\delta = 50 \mu\text{m}$ has been used for comparison purposes in part IV (20). The $\delta = 20 \mu\text{m}$ value is typical for voltammetry, PLM, and DMT experiments under well-stirred conditions. Planar diffusion with δ values in the range 20–100 μm is also applicable to metal uptake by roots or fish gills in stirred natural waters. Radial diffusion is required for biouptake by microorganisms. It can be expected, however, (5) that, in such cases, the lability of metal complexes and their corresponding contributions to the total flux will be equal to or lower than those computed for planar diffusion with

$\delta = 20 \mu\text{m}$, that is, the contribution of the free metal ion will be equal or larger.

As mentioned in the introduction, the above conditions correspond to a limiting case somewhat opposite to that corresponding to FIAM or BLM models. In the present case, maximum concentration gradients are formed at the interface, for all metal species, and their diffusion/reaction processes play a predominant role on the total flux. Note, however, that MHEDYN is not limited to the computation of the maximum flux. The more general Michaelis–Menten condition (5, 26) can be used as well.

In Parts III and IV, two important parameters are used for the interpretation of results; (a) the degree of lability ($i\xi_i$) of a complex M/L_i , for complete depletion of free M at the interphase, corresponds to the fraction of the maximum contribution of M/L_i to the flux, that is, the fraction of the contribution that would be obtained if M/L_i was fully labile (Section B in the Supporting Information and refs 13, 14, and 27); and (b) the steady-state “labile” flux, J_{lab} , is used to normalize the total computed flux at steady-state, J . J_{lab} is the flux that would be obtained if all complexes were fully labile, that is, if they were at equilibrium with M all along the diffusion layer. It is simply given by eq 1,

$$J_{\text{lab}} = \frac{\bar{D}[M]_t^*}{\delta} \quad (1)$$

where \bar{D} is the average diffusion coefficient of M , defined as (7)

$$D = \frac{D_M[M]^* + \sum_{i,j} D_{M/L_i}[M/L_i]^*}{[M]_t^*} \quad (2)$$

The major characteristics of MHEDYN are the following: the flux and concentration profile of any species can be computed in the transient and steady-state regimes, with a very large number of ligands (limited only by computer time), with rate constants and diffusion coefficients varying over many orders of magnitude, and without requirement of ligand excess compared to metal. There is no easy way to test the reliability and correctness of all results provided by this code, because no equivalent code is presently available. Tests of validation and reliability have been previously performed by comparing the results of MHEDYN with analytical solutions published in the literature for simple cases with one or two ligands (17, 18, 24).

Whenever possible, additional tests are made here by comparing the results of MHEDYN with those of another code, FLUXY (19) (available at <http://www.unige.ch/cabe/dynamic> and web.udl.es/usuaris/q4088428/Publications/Publications.html). FLUXY computes fluxes at steady state, in either planar or spherical geometry, for a very large number of ligands and for no limit of chemical rate constants and diffusion coefficients. However, it is applicable only in excess of ligands compared to metal, and successive M/L_n ($n > 1$) complexes should be in equilibrium with M/L . Comparison of the results obtained by FLUXY and MHEDYN is an additional validation test, because they are based on completely different principles. Because of the approximations made in FLUXY, analytical solutions can be reached, whereas MHEDYN, based on a numerical approach, is more general and more time-consuming. Thus, both codes are complementary.

Preliminary simulations were done with Cu-oxalate and Zn-oxalate complexes, at a spherical consuming interface simulating a microorganism, with a code developed for 3D spherical diffusion (24). The results have shown that similar and reliable results are provided by MHEDYN and FLUXY. However, they also showed that MHEDYN is significantly

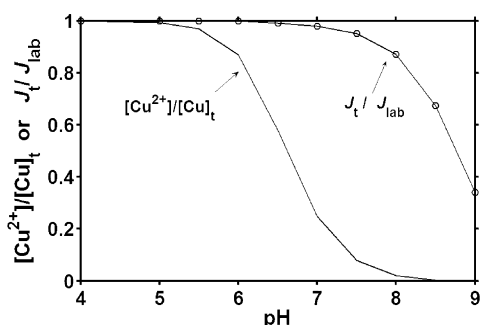


FIGURE 1. Computed total steady-state flux (J_t) normalized with respect to the labile flux (J_{lab}) and fraction of free Cu concentration as a function of pH. Other parameters: $[CO_3]_t = 2 \times 10^{-3}$ M, $[Cu]_t = 10^{-8}$ M. Full line: $[Cu^{2+}]/[Cu]_t$; Open circles: J_t/J_{lab} . The thickness of the diffusion layer is ≈ 20 μ m. Other parameters are from Table 1.

limited by computer time for 3D spherical diffusion computations, in particular when a large number of labile complexes are present. Therefore, in the present paper, simulations have been performed for planar diffusion. The corresponding version of MHEDYN is available at <http://www.unige.ch/cabe/dynamic>. Cu(II) is used as metal in this paper and in Part IV (20). The computer times needed to reach steady-state conditions, with simple ligands and fulvics (this paper) were, respectively, minutes to 1 h and 20 min to a few hours, whereas those for aggregates and mixtures of complexants (Part IV (20)) were, respectively, 20 min to a few hours and hours. Thus, for realistic aquatic systems, the computer time is non-negligible even for planar diffusion. Improvements can be done by appropriate tuning of some parameters of MHEDYN. For instance, the user can decide by himself/herself the best choice for the grid refinement factor, the size of the smallest grid, and the number of time iterations for fast reactions by using the time-splitting method. Faster computers than those used here (2Ghz Pentium 4 and 224 Mbytes of RAM) can also be employed.

3. Metal Flux in the Presence of Simple Ligands: OH^- and CO_3^{2-}

3.1. Metal Complex Distribution and Simulation Conditions. Preliminary tests have shown that, among the simple inorganic ligands and under natural conditions, OH^- and CO_3^{2-} are the most important simple ligands to study; other complexes are either not stable enough to play a significant role or are fully labile so that they do not significantly change the total flux, because their diffusion coefficients are close to or equal to that of free M. Two sets of simulations have been performed in the presence of total Cu(II) concentration, $[Cu]_t = 10^{-8}$ M; (i) at constant total carbonate concentration, $[CO_3]_t = 2 \times 10^{-3}$ M and pH varying between 4 and 9, and (ii) at constant pH = 7, 8, and 9, with $[CO_3]_t$ varying between 10^{-5} and 10^{-1} M.

Computations with MINTEQA2 (15) have shown that only the complexes $Cu(OH)^+$, $Cu(OH)_2^0$, $CuCO_3^0$, and $Cu(CO_3)_2^{2-}$ are present in significant proportions, in the bulk solution, under those conditions (Supporting Information Figure S1a–c). Steady-state metal fluxes under various conditions of pH and $[CO_3]_t$ are shown in Figures 1 and 2 (see Table 1 for the values of stability constants, diffusion coefficients, and chemical rate constants used to obtain these figures). The diffusion coefficients of all complexes are assumed to be equal to that of Cu^{2+} (7.14×10^{-10} m² s⁻¹). The values of the association rate constants, $k_{a,i}$, were computed as discussed in ref 22. Values for $k_{d,i}$ are obtained from $k_{d,i} = k_{a,i}/K_i$, where K_i is the stability constant of the complex ML_i .

3.2. Results at Constant $[CO_3]_t$ and Varying pH. Figures

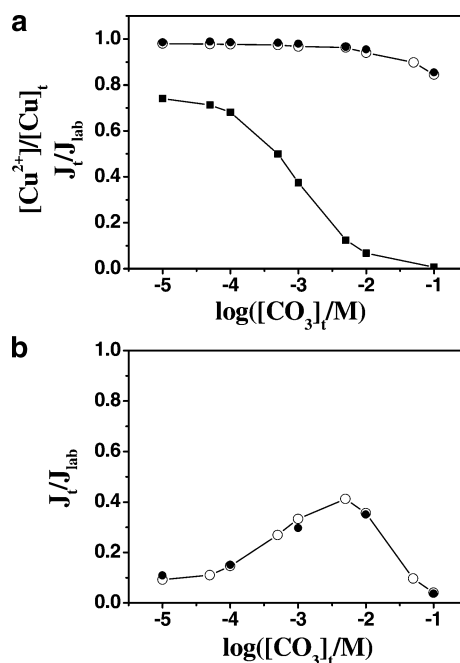


FIGURE 2. (a) Total flux normalized with respect to the labile flux as a function of $[CO_3]_t$ at pH = 7 and $[Cu]_t = 10^{-8}$ M. The fraction of free Cu in the bulk solution is given for comparison. Black squares: $[Cu^{2+}]/[Cu]_t$; Full circle: J_t/J_{lab} computed with MHEDYN; Open circles: J_t/J_{lab} computed with FLUXY. Other parameters are from Table 1. (b) Total flux normalized with respect to the labile flux as a function of $[CO_3]_t$ at pH = 9 and $[Cu]_t = 10^{-8}$ M. Full circle: J_t/J_{lab} computed with MHEDYN; Open circles: J_t/J_{lab} computed with FLUXY. Other conditions are from Table 1.

TABLE 1. Parameters Used for Cu(II) Steady-state Flux Computation in the Presence of OH^- and CO_3^{2-} ^a

species X	D_X (m ² s ⁻¹)	k_a (m ³ mol ⁻¹ s ⁻¹)	$\log K$ (m ³ mol ⁻¹)
Cu	7.14×10^{-10}		
OH	5.27×10^{-9}		
CO ₃	9.20×10^{-10}		
CuOH	7.14×10^{-10}	4.98×10^6	-7.6
Cu(OH) ₂	7.14×10^{-10}	4.15×10^6	-14.64
CuCO ₃	7.14×10^{-10}	2.31×10^7	6.75
Cu(CO ₃) ₂	7.14×10^{-10}	1.93×10^7	10.1

^a Main conditions: $T = 25$ °C, ionic strength = 0.01 M, $[Cu]_t = 10^{-8}$ M, and $\delta = 21.0$ μ m. For $Cu(CO_3)_n$, K is expressed as $K = [Cu(CO_3)_n]/[Cu][CO_3]^n$. For $Cu(OH)_n$, K is expressed as $K = [Cu(OH)_n]/[H]^n[Cu]$. Note that, because pH and carbonate are assumed to be buffered and in excess with respect to Cu(II), respectively, the diffusion processes of OH^- and carbonate ions do not influence the Cu(II) flux.

1 and S3 (Supporting Information) show the change of the total normalized flux (J_t/J_{lab}), at steady state, and the degree of lability (ξ_i) of each individual species as a function of pH for $[CO_3]_t = 2 \times 10^{-3}$ M. For comparison, Figure 1 also shows the fraction of Cu^{2+} in the bulk solution, with respect to $[Cu]_t$. If all complexes were fully labile at any pH, J_t/J_{lab} would be equal to 1 at any pH. If all complexes were inert, the curve of J_t/J_{lab} would coincide with that of $[Cu^{2+}]/[Cu]_t$. Clearly, Figure 1 shows that the behavior of the system is between these two limits, indicating that the complexes are semilabile at pH > 7.0. This is confirmed in Figure S3, which provides the degree of lability of each metal complex. For comparison, Figure S3 also shows the results obtained with FLUXY. A good agreement is obtained between the analytical solution

provided by FLUXY and the numerical solution of MHEDYN, thus confirming the validity of the results.

Supporting Information Figure S2 gives the flux contributions (j_i) of each individual complex to the total flux (J), at pH = 7. They are compared with the pH domains where each complex is predominant in the bulk solution. It is seen that at pH = 7, CuCO_3 provides the major contribution to the total flux. This is expected (12) because this complex is in dominant proportion and is fully labile (Figure S3) at that pH. At pH values larger than 8, Cu(OH)_2 becomes the largest contributor to the flux, because its proportion in solution also becomes predominant and the degree of lability of all complexes similarly decreases. $\text{Cu(CO}_3)_2^{2-}$ and Cu(OH)^+ are never important due to their low proportion (Figure S1a). A major result is that when pH increases above pH = 8, then the total flux decreases because the degrees of lability of both CuCO_3 and Cu(OH)_2 decrease (Figure S3).

3.3. Results at Constant pH and Variable $[\text{CO}_3]_t$. Figure 2, panels a and b, and Supporting Information Figure S4 show the changes of the normalized total flux (J/J_{lab}) as a function of $[\text{CO}_3]_t$, at pH = 7, 9, and 8, respectively. The results obtained with FLUXY and MHEDYN are, again, in good agreement, which confirms the validity of the results as well as the facts that (i) steady-state is reached with MHEDYN and that (ii) equilibrium between ML and ML_2 is reached for both hydroxo and carbonato complexes. Figure 2a shows that, at pH = 7, the main species contributing to the flux are labile, for most of the tested $[\text{CO}_3]_t$ concentration range. On the other hand, at pH > 8, the total flux takes maximum values when $[\text{CO}_3]_t$ is in the range 10^{-3} – 10^{-2} M (Figures 2b and Figure S4), and the total flux decreases when the pH increases. Remarkably, the Cu(II) complexes become close to nonlabile at pH > 9 (see Figure S3).

The specific reason for the maximum in the total flux at intermediate carbonate concentrations (Figures 2b and Figure S4) is an interesting question that requires a detailed study but is out of the scope of this paper. As shown in Supporting Information Figure S5, panels a and b, MHEDYN enables us to determine the effective contribution of each species to the total flux. By comparing these two figures, it is seen that at pH = 7 the major contribution to the flux is given by free Cu when $[\text{CO}_3]_t < 10^{-3}$ M and by CuCO_3 when $[\text{CO}_3]_t > 10^{-3}$ M. On the other hand, at pH = 9, the major contribution to the flux is given by Cu(OH)_2 when $[\text{CO}_3]_t < 10^{-2}$ M and by $\text{Cu(CO}_3)_2$ when $[\text{CO}_3]_t > 10^{-2}$ M. The contribution of free Cu is, then, negligible for all values of $[\text{CO}_3]_t$.

4. Metal Flux in the Presence of Fulvic Substances

4.1. Simulation Conditions. Humic and fulvic substances include an almost infinite number of analogous, but not identical, molecules that can be treated as a whole. They can be seen as an ensemble of chemically heterogeneous polyelectrolytic complexants, with rather small size distribution (21, 22). Because of chemical heterogeneity, M forms with fulvic complexing sites a very large number of different complexes (28, 29), denoted here as M/L (instead of M/S as in ref 22, where reactive sites are highlighted) for consistency in the mathematical formulation of the problem including all types of natural ligands (Supporting Information Section A). The role of these complexes in environmental systems, in particular on metal biouptake, is not clear, in particular because their dynamic behavior is ill-known. The major goals of the simulation below are (i) to determine the time required to reach the maximum steady-state flux at a consuming interface and (ii) to determine the degree of lability of the Cu(II)–fulvic complexes and their contributions to the total metal flux (J) at steady state.

It is out of the scope of this paper to describe in detail the thermodynamic and dynamic parameters of metal fulvic

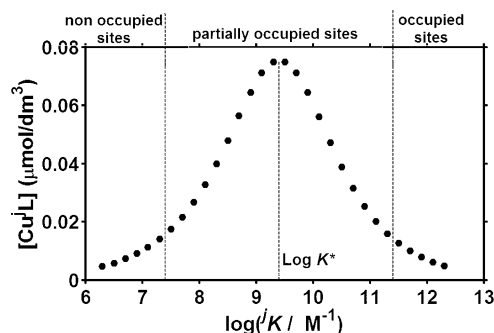


FIGURE 3. Concentration distribution of Cu–Fulvic complexes, Cu/L, in the bulk solution for the following conditions: pH = 8, $\Gamma = 0.52$, $\log K_0^* = 8.54$, $[\text{Cu}]_t = 10^{-6}$ M, $\{\text{FS}\} = 5$ mg C/dm³, and $\log jK$ ranging between 6.3 and 12.3 M⁻¹. The vertical dashed lines represent the values of $\log K^* = 9.4$, $\log K^* + 2$ and $\log K^* - 2$. They indicate the regions close to saturation and with low occupation of sites. For other parameters, see Table 2, case C.

complexes. This is discussed in refs 22, 28, and 30, and the parameters used in the present simulations have been obtained as described in ref 22. Briefly, the complexation of M with the so-called minor sites (22, 30), which are the strong sites and, thus, the most relevant for trace metals, is considered here. It has been estimated that each fulvic molecule includes not more than one such minor site (22). The thermodynamic properties of the ensemble of the minor sites are represented by a Freundlich isotherm in which metal ions are assumed to form 1/1 complexes with a very large number of different types of complexing sites having various stability constants. For the minor sites, the relationship between the molar fraction of a site type and its stability constant, is given by the so-called linear Sips distribution (e.g., refs 21 and 30) (eq 3),

$$\log j\chi = -0.174 - \log \sigma + \Gamma \log K_0^* - \Gamma \log jK \quad (3)$$

where $j\chi$ is the cumulative molar ratio of a site j , jK is the stability constant of Cu/L, σ is the total density of sites (in mol kg⁻¹) in the fulvics, and Γ and K_0^* are constants characteristic of the metal and the fulvics, respectively, at a given pH, ionic strength, and temperature. Γ is representative of the chemical heterogeneity of the fulvics. It is always comprised between 0 and 1 and is often close to 0.5. The overall complexation properties of the fulvics can also be represented by the so-called differential equilibrium function K^* (21, 22, 30), which is an average of all jK , weighted by the molar fraction and the degree of occupation of the sites jL . Thus, the value of K^* depends on the metal/ligand ratio, and it is largely controlled by the sites that are close to half-saturation (29). K^* is, thus, a useful reference parameter, which can be readily computed from experimental data (22) using eq 4,

$$\log([M_t]/\{\text{FS}\}) = \Gamma \log K_0^* - \Gamma \log K^* \quad (4)$$

where $\{\text{FS}\}$ stands for the fulvic substances mass concentration (kg/dm³). Figure 3 shows an example (corresponding to case C in Table 2) of distribution of the concentrations of complexes Cu/L as a function of $\log jK$ when the distribution function (eq 3) is discretized into classes of ligands with $\Delta \log K = 0.2$. The value of $\log K^*$ (= 9.4 in this case) is also shown on the graph. For $\log jK \gg \log K^*$ (e.g., $\log jK > \log K^* + 2$), the sites are almost fully saturated, but their number is smaller and smaller when jK increases. Thus, the corresponding $[\text{Cu/L}]$ values tend toward zero when $jK \rightarrow \infty$. For $\log jK \ll K^*$ (e.g., $\log jK < \log K^* - 2$), the complexation strength is weaker and weaker when jK decreases, and even

TABLE 2. Parameters Used and Total Fluxes Computed in Cu(II) Simulations with Fulvic Acids^a

input parameters	case A	case B	case C	case D
pH	6	6	8	8
[Cu] _t (M)	10 ⁻⁶	10 ⁻⁸	10 ⁻⁶	10 ⁻⁸
{FS} (mg C/dm ³)	5	5	5	5
[Cu] (M)	2.63 × 10 ⁻⁷	2.48 × 10 ⁻¹⁰	3.64 × 10 ⁻¹⁰	5.28 × 10 ⁻¹⁴
Ψ(mV)	-78	-78	-114	-114
δ(μm)	21.4	20.6	21.4	21.4
k _a (m ³ mol ⁻¹ s ⁻¹)	1.92 × 10 ⁷	1.92 × 10 ⁷	3.31 × 10 ⁷	3.31 × 10 ⁷
D _{FS} (m ² s ⁻¹)	2.50 × 10 ⁻¹⁰	2.50 × 10 ⁻¹⁰	2.80 × 10 ⁻¹⁰	2.80 × 10 ⁻¹⁰
Γ	0.63	0.63	0.52	0.52
log K ₀ [*]	5.06	5.06	8.04	8.04
log K [*]	6.2	9.3	9.4	13.2
computed fluxes				
J _t (mol m ⁻² s ⁻¹)	1.69 × 10 ⁻⁸	7.05 × 10 ⁻¹¹	3.15 × 10 ⁻⁹	1.32 × 10 ⁻¹³
J _{lab} (mol m ⁻² s ⁻¹)	1.76 × 10 ⁻⁸	1.27 × 10 ⁻¹⁰	1.07 × 10 ⁻⁸	1.40 × 10 ⁻¹⁰

^a T = 25 °C, ionic strength = 0.01 M, σ = 10 mol/kg C. [Cu] = free Cu concentration. The difference in values of J_{lab} between cases B and D is mainly due to the different values of diffusion coefficients of fulvics at pH 6 and 8. The difference in values of J_{lab}, between cases A and C, is partly due to the same reason, but mostly to the fact that [Cu]/[Cu]_t is significant in case A, contrary to cases B–D.

though the site concentration increases, [Cu/L] also tends toward zero at very low ⁱK values. For a given value of Γ, the shape of the curve does not depend on the conditions. Only K^{*} varies according to eq 4.

The dynamic parameters of fulvics and their complexes are given in Table 2 for the four simulated cases discussed in this paper. The diffusion coefficients of all complexes M/L are assumed to be equal to those of the fulvics themselves (D_{FS} = 2.8 × 10⁻¹⁰ m² s⁻¹ at pH = 8 and 2.5 × 10⁻¹⁰ m² s⁻¹ at pH = 6), which is a very reasonable approximation considering that the size of fulvics is much larger than that of free dehydrated M (22). The overall formation rate constants of M/L complexes (ⁱk_a) are computed, as explained in ref 22, from the rate constants for the formation and dissociation of the metal-fulvic outer-sphere complex and the rate constant for the elimination of a molecule of water from the inner hydration shell of the metal ion. The significant electrical potential inside the fulvic molecules is also considered for the formation of the outer-sphere complex, and it explains the different values of ⁱk_a at pH = 6 and 8. The dissociation rate constants (ⁱk_d) are obtained from ⁱk_d = ⁱk_a/ⁱK.

Based on the above considerations, at metal/fulvic ratios low enough for the minor sites to be dominant, the metal/fulvic solution can be seen as a mixture of complexes with widely different ⁱK and ⁱk_d values (different labilities) but with the same diffusion coefficients (same mobilities). The overall metal flux at a consuming interface is the sum of all individual fluxes. Each one mainly depends on the concentration and degree of lability (ⁱξ) of the corresponding complex. Thus, in the following, the interpretation of data will be based on the distribution curves of (i) individual fluxes, ⁱJ, and (ii) the degree of lability (ⁱξ) as a function of the stability constants of sites (ⁱK). In Figure 3 (and Figure 5, panels a and b), the log K^{*} value is given, as well as the regions of full occupation, partial occupation, and nonoccupation of sites.

Because the distributions of lability degrees and complex concentrations as function of ⁱK significantly depend on pH and metal-to-fulvic concentration ratios, their influences on the metal flux are compared for two different pH values (6 and 8) and [Cu]_t values (10⁻⁸ and 10⁻⁶ M), at constant {FS} = 5 mg C/L (Table 2). In each case A–D, the continuous distribution of sites (eq3) was discretized as discussed in refs (22) and (30), using 36, 31, 31, and 29 site types respectively, with log ⁱK values separated by a constant interval of Δ log K = 0.2. The overall tested range of log ⁱK was located

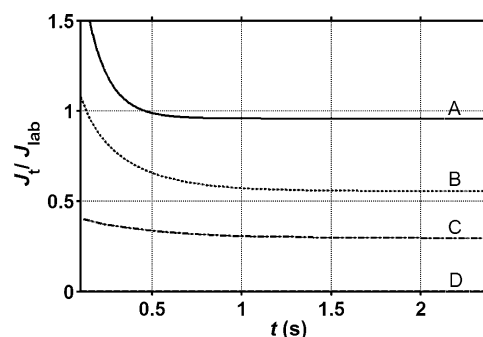


FIGURE 4. Time evolution of the total fluxes for four systems of Cu/Fulvic complexes: (A) pH = 6 and [Cu]_t = 10⁻⁶ M, (B) pH = 6 and [Cu]_t = 10⁻⁸ M, (C) pH = 8 and [Cu]_t = 10⁻⁶ M, and (D) pH = 8 and [Cu]_t = 10⁻⁸ M. In all cases, {FS} = 5 mg C/dm³. J_{lab} is the steady-state flux that would be obtained if all the complexes were fully labile. The parameters of the four simulations are listed in Table 2.

around log K^{*}, with the minimum and maximum values of log ⁱK located at log ⁱK_{min} ≤ log K^{*} - 2 and log ⁱK_{max} ≥ log K^{*} + 2, their exact values being chosen to span the largest possible range of ⁱK. The fraction of complexes outside this range is negligible (see above). However, it will be seen that their contribution to the total flux may be important.

Note that, for all sites with log ⁱK ≥ log K^{*} - 1, [L] is not in excess with respect to [M/L]. Thus, rigorous computations of fluxes cannot be performed with FLUXY, and comparison with MHEDYN is not possible in this case.

4.2. Time evolution of total flux and concentration profiles. Figure 4 gives the time evolution of the total flux (J_t) normalized with respect to the total flux at steady-state of equivalent but fully labile complexes (J_{lab}) under four pH and [Cu]_t conditions. It is seen that in all conditions, steady state is reached within 1 s or less, even for the less labile system. This suggests that, under most environmental conditions, only steady-state fluxes need to be considered, because most environmental processes occur at time scales much larger than 1 s. Figure 4 also shows that, at steady state and for sufficiently acidic pH values and large Cu(II)-to-ligand ratios (case A: pH = 6, [Cu]_t/[FS] = 0.2 mol/kg C), all the fulvic complexes practically behave as fully labile complexes. However, at higher pH and lower metal/fulvic ratios (e.g., case D: pH = 8, [Cu]_t/[FS] = 2 × 10⁻³ mol/kg C), all complexes behave as nonlabile complexes. This last result

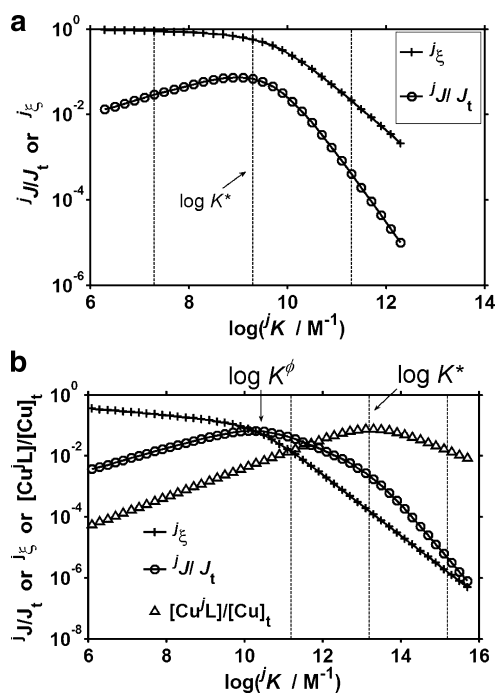


FIGURE 5. (a) Distribution of the fluxes and lability degrees of individual metal fulvic complexes, for case B: $[\text{Cu}]/[\text{FS}] = 2 \times 10^{-3}$ mol/kg C and pH = 6. The vertical dashed lines represent the values of $\log K^* = 9.3$, $\log K^* + 2$, and $\log K^* - 2$ to indicate the regions of almost full occupation, partial occupation, and very low occupation of sites (see Figure 3), respectively. Parameters used for simulation are listed in Table 2. (b) Distribution of the fluxes and lability degrees of individual Cu(II) fulvic complexes for case D: $[\text{Cu}]/[\text{FS}] = 2 \times 10^{-3}$ mol/kg C and pH = 8. The vertical dashed lines represent the values of $\log K^* = 13.2$, $\log K^* + 2$, and $\log K^* - 2$ to indicate the regions of almost full occupation, partial occupation, and very low occupation of sites (see Figure 3), respectively. The plot also shows the concentration distribution of the Cu-Fulvic complexes normalized with the total Cu concentration. Parameters used for the simulation are listed in Table 2.

is supported by a wealth of experimental data on metal/fulvic complexes (31).

Supporting Information Figure S6 shows the time evolution of the concentration profiles of three representative Cu-fulvic complexes at pH = 8 and $[\text{Cu}]_t = 10^{-6}$ M (case C), with $\log IK$ values equal to $\log K^* - 2$, $\log K^*$, and $\log K^* + 2$ respectively, that is, (i) a weak, largely labile complex, (ii) an intermediate complex, and (iii) a strong, nonlabile complex, respectively. Figure S6 shows that during the transient period the more labile complexes are depleted first at the interface, and depletion starts at longer and longer time, for less and less labile complexes. At steady state, depletion at the interface is negligible for the nonlabile complexes and increases with the degree of lability.

4.3. Distributions of Individual Fluxes and Lability Degrees, at Steady-state. Figure 5, panels a and b, and Supporting Information Figure S7 show the distributions of Ij/J_t and I_ξ for three different conditions of pH and $[\text{Cu}]/[\text{FS}]$. In Figure 5, panels a and b, $[\text{Cu}]/[\text{FS}] (= 2 \times 10^{-3}$ mol/kg C) is the same, but pH varies (pH = 6 or 8), and in Figures S7 and 5b, pH (= 8) is constant but $[\text{Cu}]/[\text{FS}]$ differs by a factor of 100. All curves show that the major contributions to the total flux are due to complexes with $\log IK < \log K^* + 1$. This is because both the proportion and the degree of lability of the complexes with $\log IK > \log K^* + 1$ are very low. The proportion of complexes with $\log IK < \log K^*$ may also be low, but their lability degree increases when $\log IK$ decreases, and at sufficiently low pH and large $[\text{Cu}]/[\text{FS}]$

values, they can be fully labile (e.g., Figure 5a). The relative roles of the proportion of a Copper complex (CuL) and its lability on the corresponding flux is better seen at high pH and low $[\text{Cu}]/[\text{FS}]$ values, where almost all complexes are nonlabile (Figure 5b). Let us call $\log K^\Phi$ the value of $\log IK$ corresponding to the maximum value of Ij/J_t . When $\log IK$ decreases from values larger than $\log K^*$, down to $\log K^*$, both the lability degree and $[\text{CuL}]$ increase, so that Ij increases sharply. When $\log IK$ decreases from $\log K^*$ to $\log K^\Phi$, $[\text{CuL}]$ decreases, but I_ξ keeps increasing. As a consequence Ij/J_t still increases, but less steeply. When $\log IK$ reaches the region where I_ξ starts to tend to an almost constant value, the decrease of $[\text{CuL}]$ is no longer compensated by the increase of I_ξ , and Ij/J_t passes through a maximum. The comparison of Figures 5, panels a and b, and Figure S7 shows that, contrary to case D (Figure 5b), in cases B and C (Figure 5a and Figure S7) the value of $\log K^\Phi$ is close to $\log K^*$. It must be realized, however, that this is fortuitous.

In all cases, the maximum flux arises always when the lability degree is at the transition between a regime where I_ξ increases when $\log IK$ decreases, to another regime where I_ξ is approximately independent of $\log IK$. This transition may occur at a $\log IK$ value quite different from $\log K^*$. Therefore, to recover the region of maximum flux in a simulation run, it is not always sufficient to explore a domain of $\log IK$ between $\log K^* - 2$ and $\log K^* + 2$, particularly in the low IK range. In some cases, it may be useful to select a limit significantly lower than $\log K^* - 2$. Overall, these results suggest that, from a dynamic point of view, one can predict that the bioavailable Cu-fulvic complexes are predominantly the weakest and intermediate ones.

Definitions of Symbols

D_{FS} , diffusion coefficient of fulvic molecules ($\text{m}^2 \text{s}^{-1}$); D_X , diffusion coefficient of species X ($\text{m}^2 \text{s}^{-1}$); \bar{D} , average diffusion coefficient of M in presence of labile complexes only; $[\text{FS}]$, total concentration of fulvics (kg C dm^{-3}); J_t , total metal flux at steady-state ($\text{mol m}^{-2} \text{s}^{-1}$); Ij , individual flux of the complex CuL ($\text{mol m}^{-2} \text{s}^{-1}$); J_{lab} , flux obtained when all complexes are assumed to be fully labile ($\text{mol m}^{-2} \text{s}^{-1}$); k_{a} , association rate constant of CuL_i ($\text{m}^3 \text{mol}^{-1} \text{s}^{-1}$); k_{d} , dissociation rate constant of CuL_i (s^{-1}); $k_{\text{a},i}$, association rate constant of CuL_i ($\text{m}^3 \text{mol}^{-1} \text{s}^{-1}$); $k_{\text{d},i}$, dissociation rate constant of CuL_i (s^{-1}); IK , stability constant of CuL ($\text{m}^3 \text{mol}^{-1}$); K^* , differential equilibrium function describing the equilibrium of the metal with the whole of fulvics; K_0^* , value of K^* when $[\text{M}]_t/[\text{FS}] = 1 \text{ mol kg}^{-1}$; $[\text{X}]^*$, bulk concentration of species X (mol m^{-3}); $[\text{X}]_t$, total concentration of species X (mol m^{-3}); Γ , constant parameters ($0 < \Gamma < 1$) describing the chemical heterogeneity of fulvics; δ , diffusion layer thickness; I_ξ , degree of lability of CuL_i ; σ , total density of sites in fulvics (mol/kg C); j_χ , cumulative molar fraction of a site j with respect to total sites in fulvics.

Acknowledgments

The Swiss National Foundation is gratefully acknowledged for its support (project No. 200020-101974/1). J. G. thanks the support from the Spanish Ministry of Education and Science (CTQ2006-14385).

Supporting Information Available

Mathematical formulation and numerical algorithm of the computer code; mathematical formulation of metal complex lability in multiligand systems, with successive complexes and without excess of ligands; figures on fluxes and lability degrees of hydroxo and carbonate complexes of Cu(II) as function of pH and carbonate concentration; figures on time evolution of concentration profiles at interface; fluxes and lability degrees of individual fulvic complexes in a Sips

distribution of complexes are provided. This information is available free of charge via the Internet at <http://pubs.acs.org>.

Literature Cited

- (1) Thibodeaux, L. J. *Chemodynamics*, Wiley-Interscience: New York, 1979.
- (2) Stumm, W. *Aquatic Chemical Kinetics*, Wiley Interscience: New York, 1990.
- (3) Campbell, P. G. C. Metal Speciation and Bioavailability in Aquatic Systems. In *IUPAC Series on Analytical and Physical Chemistry of Environmental Systems*; Tessier, A., Turner, D. R., Eds.; John Wiley & Sons: Chichester, United Kingdom, 1995; Vol. 3, pp 45–102.
- (4) van Leeuwen, H. P.; Galceran, J. Physicochemical kinetics and transport at chemical-biological surfaces. In *IUPAC Series on Analytical and Physical Chemistry of Environmental Systems*; van Leeuwen, H. P., Koester, W., Eds.; John Wiley: Chichester, United Kingdom, 2004; Vol. 9, pp 113–146.
- (5) Wilkinson, K. J.; Buffle, J. In Physicochemical kinetics and transport at chemical-biological surfaces. In *IUPAC Series on Analytical and Physical Chemistry of Environmental Systems*; van Leeuwen, H. P., Koester, W., Eds.; John Wiley: Chichester, United Kingdom, 2004; Vol. 9, pp 445–533.
- (6) van Leeuwen, H. P. Metal speciation dynamics and bioavailability: Inert and labile complexes. *Environ. Sci. Technol.* **1999**, *33*, 3743–3748.
- (7) Heyrovský, J.; Kuta, J. *Principles of Polarography*, Academic Press: New York, 1966.
- (8) Koutecký, J.; Koryta, J. The general theory of polarographic kinetic currents. *Electrochim. Acta* **1961**, *3*, 318–339.
- (9) Buffle, J.; Tercier-Waeber, M. L. Voltammetric environmental trace-metal analysis and speciation: from laboratory to in situ measurements. *TrAC, Trends Anal. Chem.* **2005**, *24*, 172–191.
- (10) van Leeuwen, H. P.; Town, R. M.; Buffle, J.; Cleven, R.; Davison, W.; Puy, J.; van Riemsdijk, W. H.; Sigg, L. Dynamic speciation analysis and Bioavailability of metals in Aquatic Systems. *Environ. Sci. Technol.* **2005**, *39*, 8545–8585.
- (11) Galceran, J.; Puy, J.; Salvador, J.; Cecilia, J.; Mas, F.; Garcés, J. L. Lability and mobility effects on mixtures of ligands under steady-state conditions. *Phys. Chem. Chem. Phys.* **2003**, *5*, 5091–5100.
- (12) Salvador, J.; Garcés, J. L.; Companys, E.; Cecilia, J.; Galceran, J.; Puy, J.; Town, R. M. Ligand mixture effects in metal complex lability. *J. Phys. Chem. A* **2007**, *111*, 4304–4311.
- (13) Salvador, J.; Garcés, J. L.; Galceran, J.; Puy, J. Lability of a mixture of metal complexes under steady-state planar diffusion in a finite domain. *J. Phys. Chem. B* **2006**, *110*, 13661–13669.
- (14) Salvador, J.; Puy, J.; Galceran, J.; Cecilia, J.; Town, R. M.; van Leeuwen, H. P. Lability criteria for successive metal complexes in steady-state planar diffusion. *J. Phys. Chem. B* **2006**, *110*, 891–899.
- (15) Allison, J. D., Brown, D. S., and Novo-Gradac, K. J. *MINTEQA2/PRODEFA2, A geochemical assessment model for environmental systems*. v. 3.0 user's manual; EPA 600/3–91/021; U.S. Environmental Protection Agency, Office of Research and Development: Washington, DC, 1991.
- (16) Tipping, E. WHAM -A chemical-equilibrium model and computer code for waters, sediments, and soils incorporating a discrete site electrostatic model of ion-binding by humic substances. *Comp. Geosci.* **1994**, *20*, 973–1023.
- (17) Alemani, D.; Chopard, B.; Galceran, J.; Buffle, J. LBGK method coupled to time splitting technique for solving reaction-diffusion processes in complex systems. *Phys. Chem. Chem. Phys.* **2005**, *7*, 3331–3341.
- (18) Alemani, D.; Chopard, B.; Galceran, J.; Buffle, J. Two grid refinement methods in the lattice Boltzmann framework for reaction-diffusion processes in complex systems. *Phys. Chem. Chem. Phys.* **2006**, *8*, 4119–4131.
- (19) Buffle, J.; Startchev, K.; Galceran, J. Computing steady-state metal flux at microorganism and bioanalytical sensor interfaces in multiligand systems. A reaction layer approximation and its comparison with the rigorous solution. *Phys. Chem. Chem. Phys.* **2007**, *9*, 2844–2855.
- (20) Alemani, D.; Buffle, J.; Zhang, Z.; Galceran, J.; Chopard, B. Metal flux and dynamic speciation at (bio)interfaces. Part IV: MHE-DYN, a general code for metal flux computation; application to particulate complexants and their mixtures with the other natural ligands. *Environ. Sci. Technol.* **2008**, *42*, 2028–2033.
- (21) Buffle, J. *Complexation Reactions in Aquatic Systems. An Analytical Approach*, Ellis Horwood Limited: Chichester, 1988.
- (22) Buffle, J.; Zhang, Z.; Startchev, K. Metal flux and dynamic speciation at (bio)interfaces. Part I: Critical evaluation and compilation of physico-chemical parameters for complexes with simple ligands and fulvic/humic substances. *Environ. Sci. Technol.* **2007**, *41*, 7609–7620.
- (23) Zhang, Z.; Buffle, J.; Alemani, D. Metal flux and dynamic speciation at (bio)interfaces. Part II: Evaluation of physico-chemical parameters and models for complexes with particulate/aggregate complexants. *Environ. Sci. Technol.* **2007**, *41*, 7621–7631.
- (24) Alemani, D. *A Lattice Boltzmann Numerical Approach for Modelling Reaction–Diffusion Processes in Chemically and Physically Heterogeneous Environments*. Ph.D. Thesis, University of Geneva, 2007.
- (25) Alemani, D.; Buffle, J.; Chopard, B.; Galceran, J. Study of three grid refinement methods in the Lattice Boltzmann framework for reaction–diffusion processes. *Int. J. Modern Phys. C* **2007**, *18*, 722–731.
- (26) Whitfield, M.; Turner, D. R. In *Chemical Modeling in Aqueous Systems*; Jenne, E. A., Ed.; American Chemical Society: Washington DC, 1979; pp 657–680.
- (27) Galceran, J.; Puy, J.; Salvador, J.; Cecilia, J.; van Leeuwen, H. P. Voltammetric lability of metal complexes at spherical micro-electrodes with various radii. *J. Electroanal. Chem.* **2001**, *505*, 85–94.
- (28) Altmann, R. S.; Buffle, J. The use of differential equilibrium functions for interpretation of metal binding in complex ligand systems: its relation to site occupation and site affinity distribution. *Geochim. Cosmochim. Acta* **1988**, *52*, 1505–1519.
- (29) Buffle, J.; Altmann, R. S.; Filella, M. The effect of physico-chemical heterogeneity of natural complexants. Part II: The buffering action and role of their background sites. *Anal. Chim. Acta* **1990**, *232*, 225–237.
- (30) Buffle, J.; Altmann, R. S.; Filella, M.; Tessier, A. Complexation by natural heterogeneous compounds: Site Occupation Distribution Function, a normalized description of metal complexation. *Geochim. Cosmochim. Acta* **1990**, *54*, 1535–1553.
- (31) Buffle, J.; Tessier, A.; Haerdi, W. In *Complexation of Trace Metals in Natural Waters*; Kramer, C. J. M., Duinker, J. C., Eds.; Martinus Nijhoff/Dr. W. Junk: Dordrecht 1984; pp 301–316.

ES071319N